

α 2,3-sialyltransferase type I regulates migration and peritoneal dissemination of ovarian cancer cells

Kuo-Chang Wen^{1,2,3}, Pi-Lin Sung^{1,2,3}, Shie-Liang Hsieh^{2,4}, Yu-Ting Chou⁵, Oscar Kuang-Sheng Lee^{2,6,7,8}, Cheng-Wen Wu^{2,9} and Peng-Hui Wang^{1,2,3,10}

¹Department of Obstetrics and Gynecology, Taipei Veterans General Hospital, Taipei, Taiwan

²Institute of Clinical Medicine, National Yang-Ming University School of Medicine, Taipei, Taiwan

³Department of Obstetrics and Gynecology, National Yang-Ming University, Taipei, Taiwan

⁴Genomics Research Center, Academia Sinica, Taipei, Taiwan

⁵Institute of Biotechnology and Department of Medical Science, National Tsing Hua University, Hsinchu, Taiwan

⁶Stem Cell Research Center, National Yang-Ming University, Taipei, Taiwan

⁷Taipei City Hospital, Taipei, Taiwan

⁸Department of Medical Research, Taipei Veterans General Hospital, Taipei, Taiwan

⁹Institute of Biomedical Science, Academia Sinica, Taipei, Taiwan

¹⁰Department of Medical Research, China Medical University Hospital, Taichung, Taiwan

Correspondence to: Peng-Hui Wang, **email:** phwang@vghtpe.gov.tw, phwang@ym.edu.tw, pongpongwang@gmail.com
Oscar Kuang-Sheng Lee, **email:** kslee@vghtpe.gov.tw, oscarlee9203@gmail.com
Cheng-Wen Wu, **email:** ken@ibms.sinica.edu.tw

Keywords: α 2,3-sialyltransferases type I, epidermal growth factor receptor, epithelial ovarian cancer, soyasaponin I

Abbreviations: EOC: Epithelial ovarian cancer; EGFR: Epidermal growth factor receptor; SsaI: soyasaponin I; OS: overall survival; ST: sialyltransferase

Received: November 10, 2016

Accepted: February 10, 2017

Published: March 07, 2017

Copyright: Wen et al. This is an open-access article distributed under the terms of the Creative Commons Attribution License (CC-BY), which permits unrestricted use, distribution, and reproduction in any medium, provided the original author and source are credited.

ABSTRACT

Epithelial ovarian cancer (EOC) has the highest mortality rate among gynecologic cancers due to advanced stage presentation, peritoneal dissemination, and refractory ascites at diagnosis. We investigated the role of α 2,3-sialyltransferase type I (ST3GalI) by analyzing human ovarian cancer datasets and human EOC tissue arrays. We found that high expression of ST3GalI was associated with advanced stage EOC. Transwell migration and cell invasion assays showed that high ST3GalI expression enhanced migration of EOC cells. We also observed that there was a linear relation between ST3GalI expression and epidermal growth factor receptor (EGFR) signaling in EOC patients, and that high ST3GalI expression blocked the effect of EGFR inhibitors. Co-Immunoprecipitation experiments demonstrated that ST3GalI and EGFR were present in the same protein complex. Inhibition of ST3GalI using a competitive inhibitor, Soyasaponin I (SsaI), inhibited tumor cell migration and dissemination in the *in vivo* mouse model with transplanted MOSEC cells. Further, SsaI synergistically enhanced the anti-tumor effects of EGFR inhibitor on EOC cells. Our study demonstrates that ST3GalI regulates ovarian cancer cell migration and peritoneal dissemination via EGFR signaling. This suggests α 2,3-linked sialylation inhibitors in combination with EGFR inhibitors could be effective agents for the treatment of EOC.

INTRODUCTION

Epithelial ovarian cancer (EOC) is the second most common type of gynecologic cancer and a leading cause of gynecological cancer deaths in the United States. In 2016, there were 14,240 EOC related deaths and 22,280 new cases diagnosed in the United States [1]. Despite intensive treatment with cytoreductive surgery and post-operative adjuvant chemotherapy with/without anti-angiogenesis agents, EOC has the highest mortality rate among gynecological cancers because it is diagnosed in an advanced stage and has high recurrence rate [2-4]. The estimated average disease-free survival (DFS) time for EOC patients is 18 months with a 5-year overall survival (OS) rate below 30% [5]. EOC is characterized by advanced-stage presentation, multiple organ metastases, peritoneal dissemination and refractory ascites at diagnosis [6]. Currently, the diagnosis of metastasis and/or recurrence is still dependent on imaging clues and detection of carbohydrate antigen 125 (CA125) [7], both of which are limited in sensitivity and specificity. Therefore, the development of novel biomarkers is urgently required for accurate and early prediction of metastasis and treatment outcomes in EOC patients.

Sialic acids belong to a family of 9-carbon amino sugars that are widely distributed in nature as terminal sugars of oligosaccharide chains of glycoconjugates (glycoproteins and glycolipids) [8]. The sialyltransferases (ST) and sialidases regulate sialylation, which is an important posttranslational modification reported during progression of many cancers [9-11]. The ST family consists of three subfamilies with 20 anabolic enzymes [12], namely, α 2,3-sialyltransferases that mediate the transfer of sialic acid with an α 2,3-linkage to terminal Gal residues (ST3GalI-VI) and α 2,6-sialyltransferases that mediate the transfer of sialic acid with an α 2,6-linkage to terminal Gal (ST6GalI-II) or GalNAc residues (ST6GalNAcI-VI) [13, 14]. The link between the ST family and EOC was reported previously by few studies [15-17]. For example, Christie *et al* reported that sialylation of β 1 integrins mediated by ST6Gal-I altered the adhesion and migration characteristics of ovarian cancer cells through the extracellular matrix leading to peritoneal metastasis [17].

In our previous study, we showed altered expression and significant increase of α 2,3-linked sialylated proteins in ovarian cancer patients and the enhanced α 2,3-linked sialylation was directly linked to increased expression of ST3GalI [16]. The competitive ST inhibitor, soyasaponin I (SsaI, $K_i = 2.3\mu\text{M}$) was shown to affect CMP-Neu5Ac binding to ST, but did not inhibit other glycosyltransferases and glycosidases [18]. Further, SsaI inhibited α 2,3-linked sialic acid expression in B16F10 melanoma and MDA-MB-231 breast cancer cell lines that resulted in increased adhesion and decreased migration and invasiveness of the two cell lines [19, 20].

Epidermal growth factor receptor (EGFR), also known as ErbB-1 or HER1, is a transmembrane receptor tyrosine

kinase (RTK) and a member of the human epidermal receptor (HER) family, which is involved in many cell signaling pathways. EGFR is overexpressed in many cancers and regulates cancer invasion, metastasis, and angiogenesis [21-25]. After binding to specific ligands (EGF or TGF- α), EGFR undergoes conformation changes and forms homo- or hetero-dimers with other HER family members [26-31]. After autophosphorylation, the dimeric EGFR recruits and activates various downstream cytoplasmic and nuclear signaling proteins, which regulate multiple cellular processes, including proliferation, migration, differentiation, survival, and apoptosis [26-28]. Overexpressed EGFR is associated with poor prognosis in ovarian cancers [32-34]. Although EGFR is an attractive therapeutic target, clinical trials with several EGFR inhibitors have demonstrated modest anti-tumor effects on ovarian cancer [34-36]. Therefore, in this study, we investigated the prognostic value of ST3GalI and its relationship with EGFR signaling in ovarian cancer using both *in vitro* and *in vivo* models including human ovarian cancer patient microarray datasets.

RESULTS

ST3GalI is a prognostic factor for migration and peritoneal dissemination of human ovarian cancer cells

First, we analyzed the correlation between overall survival (OS) rate and expression data of sialyltransferases (high, moderate or low) using the Human Genome U133A Array (562 tumor cases) available from The Cancer Genome Atlas (TCGA) at the OncoPrint website. We observed that ST3GalI played a more critical role in disease progression than ST6GalI (α 2,6-sialyltransferase) and ST8SIAI (α 2,8-sialyltransferase). Kaplan-Meier analyses of TCGA cohort specimens showed that EOC patients with high ST3GalI expressing tumors demonstrated poor survival rates (Figure 1A and Table 1). Furthermore, immunohistochemical (IHC) staining using the human EOC tissue array (CJ2 provided by SUPER BIO CHIPS, Seoul/South Korea) showed that higher intensity staining of ST3GalI (Figure 1B) positively correlated with lower overall survival rate (Figure 1C). These findings demonstrated that ST3GalI had significant prognostic value in human ovarian cancer.

We further investigated the association of ST3GalI expression with EOC progression. Compared to early stages, ST3GalI expression was significantly higher in advanced stages among the various ovarian cancer datasets tested (Supplementary Figure 1A). This suggested that overexpression of ST3GalI was associated with advanced stage EOC (peritoneal seeding and distant metastases), especially in advanced serous- or clear-type cell carcinoma (Supplementary Figure 1B).

Further, we investigated the role of ST3GalI in ovarian cancer cell migration by either knocking

down or overexpressing ST3Gal I in human ovarian cancer ES2 cells and performing Transwell assays. We observed that downregulation of ST3Gal I significantly suppressed cancer cell migration and invasion, whereas overexpression of ST3Gal I enhanced cell migration and invasion (Figure 1D–1E, and Supplementary Figure 2). Interestingly, altered ST3Gal I expression (knockdown or overexpression) did not significantly affect tumor growth

(Supplementary Figure 3). These findings suggested that ST3Gal I regulated the migration and invasiveness of ovarian tumor cells without altering tumor growth.

ST3Gal I interacts with EGFR signaling pathway in ovarian cancer

To identify the signaling pathways regulated by ST3Gal I, we analyzed important cell receptors in the

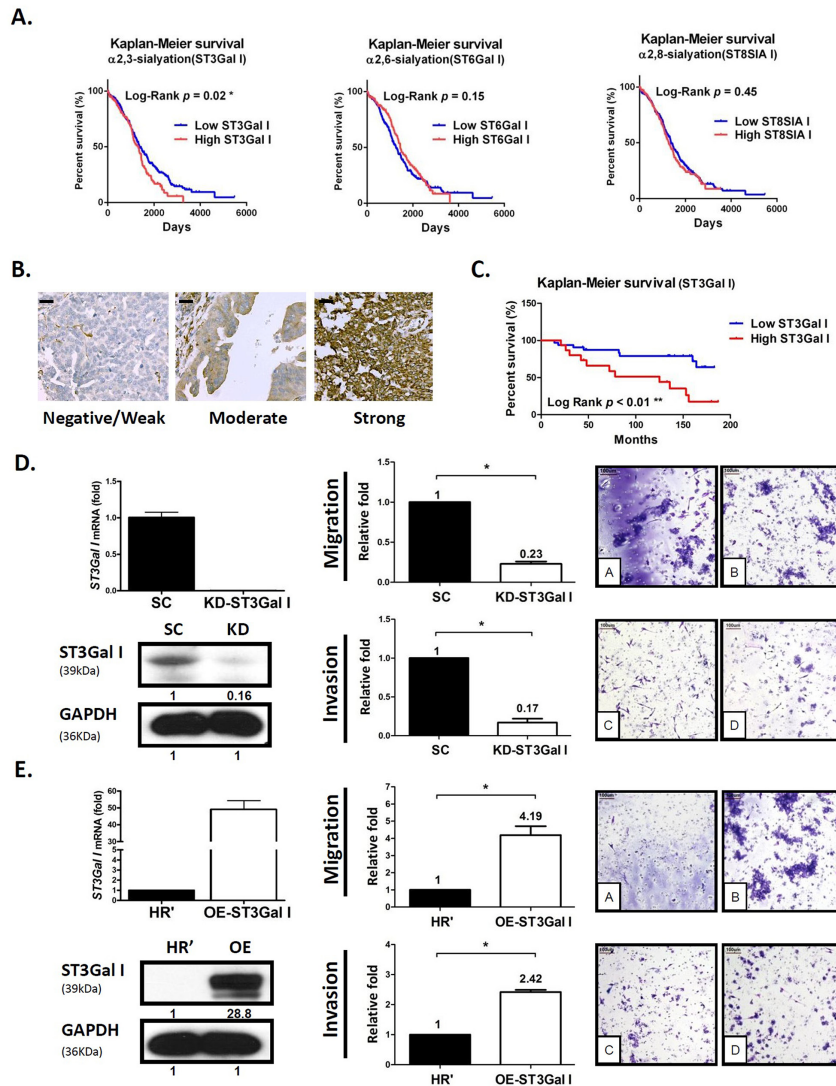


Figure 1: ST3Gal I is a prognostic factor for tumor migration and peritoneal dissemination of human ovarian cancer. (A) Using Oncomine TCGA ovarian cancer genomics (562 ovarian carcinoma samples analyzed on an Affymetrix Human Genome U133 array; 12,624 measured genes), we compared different ST mRNAs, including α 2,3-, α 2,6-, and α 2,8-linked ST, with survival time using a tertile approach. Patients with an upper one-third mRNA expression were defined as the high subgroup, while others with lower two-thirds mRNA expression were defined as the low subgroup. (B–C) IHC analysis of ST3Gal I was performed on commercial human ovarian cancer tissue array samples (Super Bio Chips, CJ2, Korea). The intensity scores were as follows: 0, no staining; 1, weak; 2, moderate; 3, strong. Low ST3Gal I included weak, moderate or no staining; high ST3Gal I was defined as strong staining. Scale bars representing 20 μ m were added from an image taken at identical magnification and resolution. The percentage was determined in the early stage (FIGO stage I & II) or late stage (FIGO stage III&IV) disease groups. The Fisher’s exact test was used to statistically analyze the percentage for the early and late stages. Kaplan-Meier survival curves were used to analyze OS in low- and high-ST3Gal I groups. (D–E) Transwell migration and matrigel invasion of ES2 human ovarian cancer cells with either ST3Gal I knocked-down or over-expressed was assayed. Total numbers of cells in 7 random fields were counted. Data shown are the mean \pm SD of 3 separate experiments (*: $p < 0.05$, **: $p < 0.01$). Data on the Y-axis represented relative value compared to control. Immunoblots were quantified using Image J software.

Table 1: Overall survival time in different sialyltransferases of TCGA human ovarian cancer

Sialyltransferase	Overall survival time (Days)			
	Low expression (n=376)	High expression (n=186)	p-value	
α2,3-sialylation	ST3GAL I	1042.1±88.0	921.7±93.8	0.02 *
	ST3GAL II	993.2±82.1	1020.6±114.6	0.99
	ST3GAL IV	969.3±81.3	1068.8±116.2	0.28
	ST3GAL V	1005.1±83.1	996.4±111.5	0.38
	ST3GAL VI	993.9±81.3	1019.1±117.1	0.27
	ST6GAL I	942.7±82.7	1122.6±110.8	0.15
α2,6-sialylation	ST6GALNAC II	955.7±77.5	1096.3±126.0	0.39
	ST6GALNAC IV	1016.8±84.5	972.7±106.9	0.61
	ST6GALNAC V	961.0±81.0	1085.6±116.6	0.62
α2,8-sialylation	ST8SIA I	1006.1±85.8	994.5±103.1	0.45
	ST8SIA II	988.0±81.6	1030.9±115.8	0.22
	ST8SIA III	979.6±82.6	1048.0±112.8	0.56
	ST8SIA IV	1007.8±83.3	991.0±111.0	0.49
	ST8SIA V	983.2±81.9	1040.8±115.2	0.86

* Kaplan Meier overall survival analysis

human ovarian cancer ES2 cell line using the L1000 mRNA microarray. Our analysis showed that ST3GalII expression was significantly associated with expression of the EGFR genes (Figure 2A). Also, the EGFR signaling pathway was overexpressed and associated with poor prognosis in more than 70% of ovarian cancer patients [32]. We further analyzed three ovarian cancer genomic datasets (TCGA, Bittner, and Lu) and found a linear relationship between ST3GalII and EGFR (Figure 2B, upper panel). We observed that ovarian cancer patients with a high ST3GalII expression demonstrated increased EGFR levels simultaneously (Figure 2B, lower panel). Further, the patients that highly expressed ST3GalII and EGFR simultaneously, demonstrated poorer clinical prognosis than others (Supplementary Figure 4A). Moreover, there was a close relationship among different subtypes of EOC such as serous carcinoma (Pearson $r = 0.25\text{--}0.58$, $p < 0.01$, Supplementary Figure 4B–4C).

Next, we analyzed the mRNA levels of the different STs, namely, ST3GalII–VI in response to EGFR inhibitor treatments (erlotinib, lapatinib, ZD-6474, TKI258) in different ovarian cancer cell lines listed in the Cancer Cell Line Encyclopedia (CCLE) database. We observed that the anti-tumor effect of EGFR inhibitors was more pronounced when the mRNA expression of STs was lower (Figure 2C, left side of heat-map). However, EGFR inhibitors demonstrated poorer anti-tumor effect in cell lines with higher expression of STs (Figure 2C, right side of heat-map). These results demonstrated synergy between ST3GalII levels and EGFR.

To understand the relationship between ST3GalII and EGFR, we investigated the EGFR expression in the ovarian cancer cells with ST3GalII either knocked down or overexpressed. We observed that ST3GalII knock down decreased EGFR expression, whereas ST3GalII overexpression enhanced EGFR levels (Figure 2D–2E). In addition, we observed that ST3GalII associated with epithelial mesenchymal transition (EMT) markers, such as E-cadherin or N-cadherin (Supplementary Figure 5) since we observed increased E-cadherin and decreased N-cadherin in the ST3GalII knock-down. Co-Immunoprecipitation analysis demonstrated that EGFR and ST3GalII were physically present in the same protein complex since ST3GalII was found in the complex immunoprecipitated from ES2 ovarian cancer cell lysates with anti-EGFR antibodies and EGFR was immunoprecipitated with anti-ST3GalII antibody (Figure 2F). Further, in the ST3GalII knock-down, we observed decreased ST3GalII immunoprecipitating with anti-EGFR antibody (Figure 2G). Interestingly, we also observed that ST3GalII regulated EGFR transcriptionally in a time-dependent manner (Figure 2H). We observed that when ST3GalII was down regulated by shRNA knockdown, an immediate and profound reduction of ST3GalII expression was followed by a stable and longer down regulation of EGFR. This finding suggested that ST3GalII may regulate the EGFR pathway via regulate factors that were upstream of EGFR in the signaling pathway or even a negative feedback mechanism. Taken together, these findings suggested that ST3GalII positively regulated EGFR.

α 2,3-sialylation inhibitor SsaI suppresses ovarian cancer cell migration and peritoneal dissemination

Next, we investigated if the α 2,3-sialylation inhibitor, SsaI, inhibited peritoneal seeding and carcinomatosis

of ovarian cancer and the mechanism by which SsaI modified the behavior of cancer cells. We observed that SsaI treatment down regulated ST3GalI in three ovarian cell lines (MOSEC, ES2, and OVCAR3) compared to the DMSO control (Figure 3A). Further, Transwell assay demonstrated that SsaI treated MOSEC, ES2, and OVCAR3 ovarian cancer cells demonstrated significant inhibition of

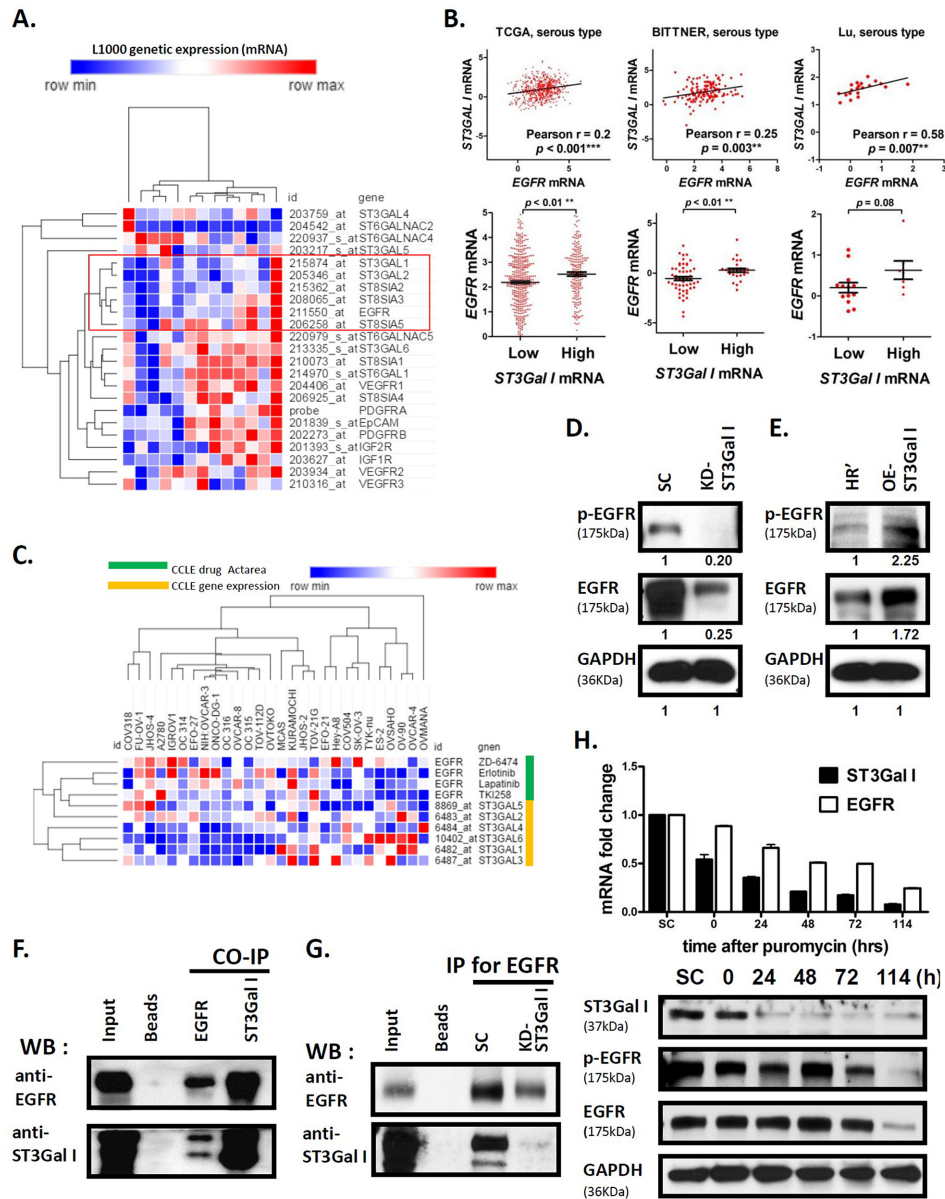


Figure 2: ST3GalI interacts with EGFR signaling pathway in ovarian cancer. (A) The correlation of 20 STs and significant cell receptors in the ES2 ovarian cancer cell line were analyzed by the L1000 mRNA microarray. Data shown are mean \pm SD of separate repeat experiments. (B) The analysis of mRNA expression of ST3GalI and EGFR from Oncomine TCGA (n=562), Bittner (n=241), and Lu (n=50) ovarian cancer genomics is shown. The expression of EGFR was compared between low and high ST3GalI groups using a tercile approach. (C) The mRNA expression of α 2,3-sialyltransferases and TKI drug efficiency (Actarea) are shown from the CCLE ovarian cancer dataset. (D-E) Western blot analysis of EGFR and phospho-EGFR in ST3GalI knocked-down or overexpressing cells compared to controls is shown. GAPDH was used as control (same GAPDH as in Figure 1D-1E). (F) The co-immunoprecipitation assay coupled with immunoblotting analysis to evaluate the protein-protein interaction of ST3GalI and EGFR is shown. (G) Immunoblotting of ST3GalI immunoprecipitated with anti-EGFR antibodies in SC and ST3GalI knock-down of ES2 cell line are shown. (H) Time course RNA and protein analysis showing EGFR expression during ST3GalI knock-down.

motility (Figure 3B). These results indicate that ST3GalI may regulate tumor cell motility and hence a potential prognostic marker of human ovarian cancer. More than half

of ovarian cancer patients are found in an advanced stage where the ovarian cancer cells have disseminated into the peritoneal cavity to form peritoneal seeding and sometimes

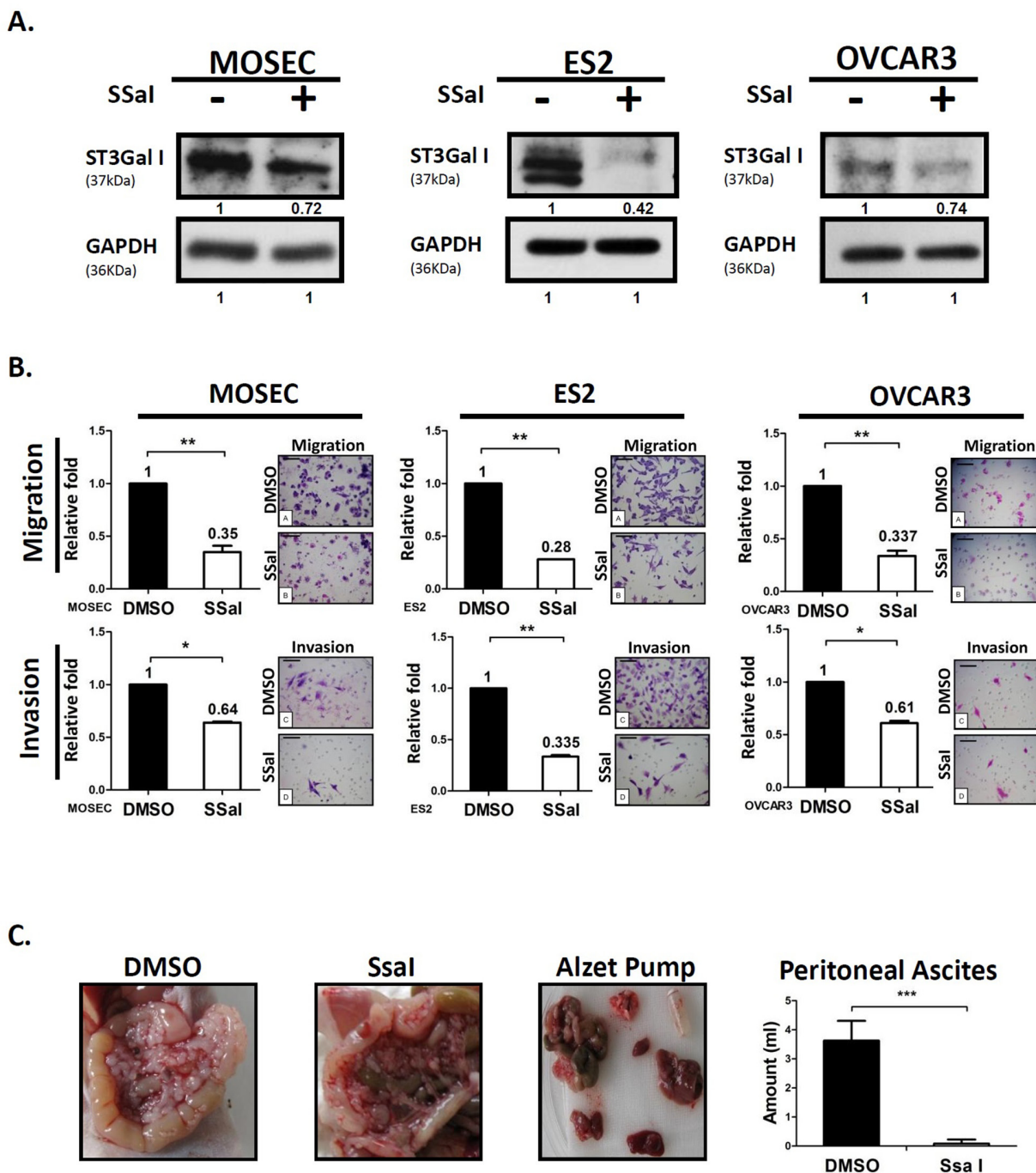


Figure 3: α 2,3-sialylation inhibitor Ssal suppresses ovarian cancer tumor migration and peritoneal dissemination.

(A) Quantification of ST3GalI in ovarian cancer cells (MOSEC, ES2, and OVCAR3) treated with 100 μ M Ssal or DMSO control for 72h by western blot; GAPDH was used as internal control. (B) The Transwell migration (upper panel) and invasion assay (low panel) on ovarian cancer cells that were stained with Toluidine blue and Crystal violet solution, respectively. Data shown are the mean \pm SD of 3 separate experiments. (C) MOSEC cells (2×10^6) were injected into the peritoneal cavity of 8weekold female C57BL/6 mice ($n=10$). ALZET Micro-Osmotic Pumps were filled with either 100 μ M Ssal or DMSO as control was implanted subcutaneously. The mice were sacrificed after 4 weeks and the amount of ascites was measured. The body weights of mice were recorded after injecting MOSEC cells and implantation of pumps implantation. Data shown are the mean \pm SD of 5 mice. Peritoneal seeding and carcinomatosis were analyzed in the Ssal and DMSO control groups. (*: $p < 0.05$, **: $p < 0.01$, ***: $p < 0.001$.)

carcinomatosis. To investigate this, we injected MOSEC cells into the peritoneal cavity of 8 week-old female C57BL/6 mice along with continuous delivery of either 100 μ M SsaI or DMSO control from ALZET Micro-Osmotic pumps. We observed peritoneal carcinomatosis with a large amount of ascites in the control mice, mimicking the clinical symptoms of human ovarian cancer (Figure 3C). In contrast, the SsaI-inoculated mice were asymptomatic and demonstrated significantly lower peritoneal carcinomatosis and ascites (Figure 3C). Interestingly, SsaI mildly inhibited cell proliferation in the MOSEC cell line as analyzed by MTT assay (Supplementary Figure 6A), and showed negligible decrease in mouse body weight (Supplementary Figure 6B). Taken together, these data suggested that SsaI, the ST3GalII inhibitor, significantly reduced tumor migration and peritoneal dissemination without significantly affecting growth.

SsaI inhibits EGFR signaling and shows synergistic effect with TKI

To examine if SsaI inhibited the EGFR signaling pathway through ST3GalII, we treated the ovarian cancer cell lines with SsaI and found that EGFR expression was down-regulated (Figure 4A). Besides inhibiting the sialylation of EGFR, SsaI interfered with the protein-protein interaction between ST3GalII and EGFR. The intraperitoneal tumor tissues from the B6 mice that were treated with SsaI showed decreased expression of ST3GalII and EGFR compared to the control mice based on DuoLink *in situ* double staining (Figure 4B). This suggested that SsaI suppressed tumor migration and peritoneal dissemination in ovarian cancer via ST3GalII-EGFR signaling.

Further, we investigated the synergy between ST3GalII and EGFR. Towards this, we treated ES2 cells with SsaI in presence or absence of the EGFR inhibitor, AG1478. We observed that cells treated with both SsaI and AG1478 showed significant inhibition of tumor invasion in the Transwell invasion assay compared to cells treated with SsaI alone or the negative control (Figure 4C). Also, we noted that EGF stimulation was suppressed by SsaI treatment in the Transwell matrigel assay (Supplementary Figure 7). Moreover, we demonstrated synergistic effects of the SsaI and AG1478 inhibitor combination over several concentrations (Figure 4D, Table 2). Hence, these data demonstrated that α 2,3-sialylation inhibitors may be useful in future ovarian cancer therapy to synergize with TKI (tyrosine kinase inhibitors).

DISCUSSION

Cell surface glycans are induced during carcinogenesis suggesting that they are involved in human cancers [37]. The sialyltransferases (STs) are classified based on the position of attachment of the donor sialic acid

to the acceptor as either α 2,3 (ST3), α 2,6 (ST6) or α 2,8 (ST8), and based on their acceptor specificity (for example, ST3GalI, ST3GalII, etc). The STs catalyze transfer of the sialic acid moiety from a cytidine-5'-monophospho-*N*-acyl-neuraminic acid donor (CMP-Neu5Ac) to the various acceptor glycoconjugates terminating in either galactose (Gal), *N*-acetylgalactosamine (GalNAc) or another sialic acid [38, 39].

ST3GalII is specific for α 2,3-sialylation of Gal β 1, 3GalNAc on the O-linked chains of glycoproteins and glycolipids and has an important role in sialyl-Lex/Lea biosynthesis and sialylation of the Thomsen-Friedenreich antigen [40-42]. In previous studies, the expression of ST3GalII was altered in cancers such as colon, bladder, ovary and breast cancer [43]. Videira *et al* found that the overexpression of ST3GalII was associated with the initial oncogenic transformation of bladder [44]. Kudo *et al* showed that ST3GalII was up-regulated in colorectal cancer [45]. Burchell *et al* showed that ST3GalII was elevated in primary breast carcinomas, compared to normal or benign breast tissues [43]. In our previous work, we found that increased ST3GalII expression contributed directly to increased α 2,3-linked sialylation in ovarian serous carcinoma [16]. Therefore, in this study we investigated the mechanistic role of ST3GalII in ovarian cancer. Initially, we investigated the relationship between ST3GalII expression, advanced cancer stage and overall survival rate. Using different microarray datasets, we found that ST3GalII was significantly higher in late-stage cancer patients compared to early-stage cases. Furthermore, *in vitro* and *in vivo* studies revealed that ST3GalII down regulation significantly suppressed cancer cell migration and invasion. Conversely, ST3GalII overexpression enhanced the migratory ability and invasiveness of the cancer cells. Taken together, our data demonstrated that ST3GalII played a significant role in ovarian cancer cell migration and peritoneal dissemination and suggested a potential prognostic role.

Since enhanced sialylation was observed in oncogenic transformation, tumor metastasis, and invasion, inhibition of ST may be a potential treatment strategy. A cell permeable ST inhibitor, SsaI, exhibited inhibition of cellular α 2,3-sialyltransferase activity [18, 46]. Our previous study showed that SsaI significantly decreased breast cancer cell (MDA-MB-231) migration [19, 20]. In the present study, we demonstrated inhibitory effects of SsaI on migration and invasion of ovarian cancer cell lines, as well as decreased peritoneal tumor ascites in mice. Interestingly, SsaI downregulated the expression of ST3GalIV in breast cancer cells and not ST3GalI and ST3GalIII [19, 20], but inhibited ST3GalII in ovarian cancer cells. This suggested a probable negative feedback regulation of ST3GalII that needs to be investigated along with the ability of SsaI to inhibit different STs in different cancer types.

Studies on non-small—cell lung cancers and others have revealed that several mechanisms like mutation (T709M) of EGFR receptors or activation of alternative signaling pathways or sialylation regulate EGFR function and inhibitor resistance [47-50]. Further, studies found

that Asn420 and 579on the glycans prevented ligand-independent dimerization of EGFR [51-53]. Liu *et al* showed that sialylation and fucosylation suppressed dimerization and autophosphorylation of EGFR and EGF-induced lung cancer cell invasion [54]. Yen *et al* showed

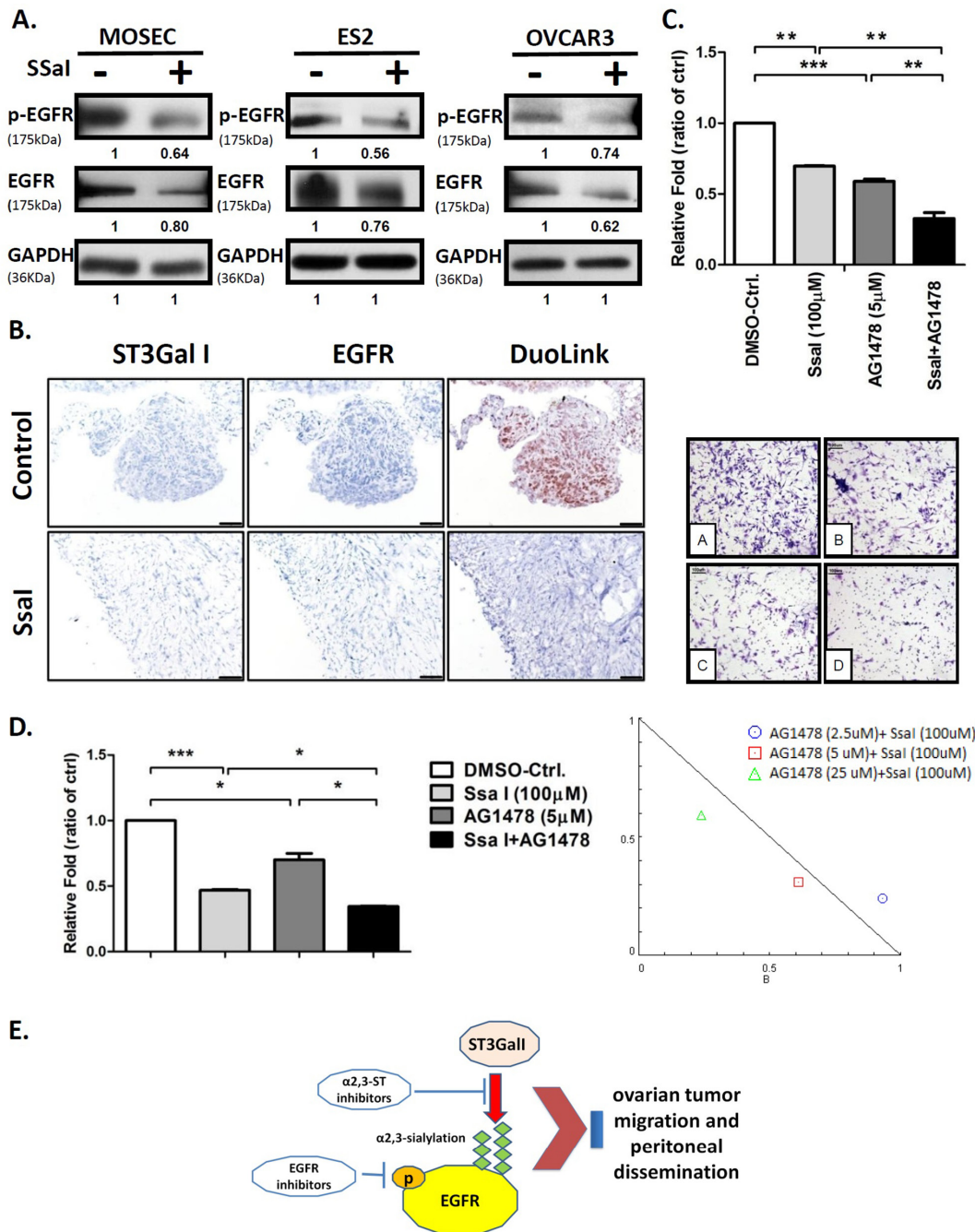


Figure 4: α2,3-sialylation inhibitor SsaI affects EGFR signaling and synergizes with TKI. (A) Quantification of EGFR and phospho-EGFR in ES2 cells treated with 100μM SsaI or DMSO control for 72h; GAPDH was used as control (same GAPDH as in Figure 3). **(B)** Intraperitoneal tumors from B6 mice treated with either SsaI or DMSO control were stained by the Duolink *in situ* IHC staining kit to analyze for ST3GalI and EGFR. **(C)** ES2 cells were treated with 100μM SsaI and 5μM AG1478 (EGFR inhibitor) were subjected to Transwell matrigel invasion assay. Total numbers of cells were counted in 7 to 10 random fields. Data shown are the mean ± SD of 3 separate experiments. **(D)** Synergy between ST3GalI and EGFR were determined by treating ES2 cells with either SsaI or AG1478 (EGFR inhibitor) or both for 48h followed by determination of their effects on cell proliferation rate. Data shown are the mean ± SD of 3 independent experiments. **(E)** A proposed mechanism of the interaction between ST3GalI and the EGFR signaling pathway.

Table 2: Synergistic effects of SsaI and EGFR inhibitor

SsaI (μM)	AG1478 (μM)	CI*
100	2.5	1.17
100	5	0.92
100	25	0.84
25	25	0.78
25	50	0.57

* Combination index (CI) is a quantitative measure of the degree of interaction between different drugs. If CI =1, it denotes additivity; if CI > 1, it denotes antagonism; and if CI < 1, it denotes synergism.

that sialylation partially suppressed the phosphorylation of EGFR at Y1068, Y1086, and Y1173 in a TKI-resistant lung cancer cell line with L858R/T790M mutations on EGFR and enhanced EGFR sensitivity to TKI [30]. Therefore, in contrast to lung cancer, our data with ovarian cancer cells suggested that sialylation was positively associated with EGFR function. Further, our co-IP data demonstrated that ST3GalII and EGFR interacted with each other (Figure 2F and 2G), and EGFR expression decreased in the ST3GalII knocked-down cell line. Interestingly, ST3GalII also regulated the transcription of EGFR (Figure 2H). These data demonstrated that sialylation in ovarian cancer may be functionally different than in lung cancer.

There are limitations to our study. First, only serous histology was available in the TCGA dataset and small number of case studies in other genomic datasets. Therefore, a larger-scale investigation of different histologic types in ovarian cancer is necessary. Second, previous studies showed that SsaI was a competitive inhibitor of CMP-Neuc5Ac, but, we found that SsaI down-regulated ST3GalII. This implied that SsaI suppressed α 2,3-sialylation via a negative feedback regulation that needs to be investigated further. Third, although the results showed that α 2,3-sialyltransferases increased EGFR expression in EOC, the effect of sialylation on EGFR structure or conformation was not directly explored. Moreover, the detailed mechanism by which ST3GalII regulated EGFR is not clear in this study. A marked reduction of ST3GalII expression was observed soon after transfection with the ST3GalII knock-down plasmid, whereas EGFR down regulation as a consequence was found to be relatively stable and long-lived. This implied that ST3GalII may regulate factors upstream of EGFR or induce a negative feedback inhibition of EGFR signaling pathway. Fourth, we used only one EGFR inhibitor, AG1478, which is a specific reversible inhibitor of EGFR that selectively inhibits the ligand-induced autophosphorylation of EGFR and downstream signal transduction events [55]. Moreover, this compound has not been evaluated in clinical trials. Other EGFR inhibitors such as gefitinib,

erlotinib, lapatinib and anti-EGFR antibodies that are used in cancer therapy need to be considered in combination with ST inhibitors and their efficacy and safety for ovarian cancer patients needs to be evaluated.

In conclusion, our study showed that ST3GalII was a poor prognostic factor in epithelial ovarian cancer (EOC), especially with regard to survival and metastasis. We demonstrated crosstalk between ST3GalII and EGFR that regulated the migration and invasiveness of ovarian cancer cells. Further, our study demonstrated that α 2,3-linked sialylation inhibitors such as SsaI in combination with EGFR inhibitors may be potentially future therapeutic targets for EOC treatment.

MATERIALS AND METHODS

Cell culture

The human ovarian carcinoma cell line, ES-2, was cultured in McCoy's 5A medium supplemented with 10% FBS and 1% penicillin-streptomycin. The human ovarian carcinoma cell line, OVCAR-3, was cultured in DMEM/F12 medium supplemented with 10% fetal bovine serum (FBS), 1% non-essential amino acids, 1% sodium pyruvate, 1% L-glutamine and 1% penicillin-streptomycin. The mouse ovarian surface epithelial cell line, MOSEC, was cultured in RPMI1640 supplemented with 10% FBS, 1% non-essential amino acid, 1% sodium pyruvate, 1% L-glutamine, 0.1% beta-mercaptoethanol (beta-ME) and 1% penicillin-streptomycin. All the cells were incubated at 37°C and at 5% CO₂.

Thiazolyl blue (MTT) assay

To estimate cell survival and proliferation, the ovarian cancer cell lines (5×10^3) were grown in RPMI1640 medium in 96 well plates supplemented with 5% charcoal-stripped/heat-inactivated FCS for 24h. Then, the cells were treated with either DMSO (control) or 100 μM SsaI (Soyasaponin I, S9951 Sigma Soyasaponin I Sigma-Aldrich) for 48h. Further, 200 μl thiazolyl blue (MTT, 5mg/ml, Sigma-Aldrich) was added into each well with 1ml of medium for 4h at 37°C followed by 2 ml of 0.04N HCl in isopropanol. After thorough mixing by pipetting and 5 min of incubation at room temperature, the absorbance was read at 570nm and subtracted from background absorbance at 600nm. Results were expressed as the mean \pm SD of 3 independent experiments.

Cell migration assay

Transwell cell migration assay was used to estimate the effect of SsaI on the migration of the ovarian tumor cells. The Transwell consisted of an upper and a lower chamber that were separated by a polycarbonate filter of 8 μm pore size with a surface diameter of 6.5mm. The ovarian cancer

cells (2×10^4) were added to the upper chamber in serum free medium with either DMSO (control) or $100\mu\text{M}$ SsaI. The lower chamber was filled with 10% FBS that served as a chemoattractant. After incubation at 37°C for 4h, the non-migratory cells from the upper surface of the filter were removed with wet cotton swabs. Then, cells that had migrated to the lower surface of the filters were fixed, stained with DAPI ($1.0\mu\text{g}/\text{ml}$) and then counted from 7 to 10 random fields of view at $400 \times$ magnification. The data were expressed as the average number of cells per field.

Cell invasion assay

In vitro invasiveness of the ovarian cancer cells was assessed by quantifying the number of cells that invaded the Matrigel. Polycarbonate Transwell filters was coated with $\sim 100\mu\text{g}/100\mu\text{L}$ of diluted Matrigel solution. Then, the cells (2×10^4) were added to the upper chamber with either DMSO or $100\mu\text{M}$ SsaI and 10% FBS medium was added as a chemoattractant in the lower chamber followed by incubation at 37°C for 24 h. The cells that travelled through the filter were stained and counted from 7 to 10 random fields of view at $400 \times$ magnification.

Soyasaponin I preparation

SsaI was prepared from a commercial preparation of soybean saponins. The purification process was performed as described with some modifications. Briefly, non-saponin constituents were extracted from the preparation by gently agitating the saponins (4g) in acetone (25ml) at room temperature followed by centrifuging the mixture at $2000 \times g$ for 30 min. This acetone extraction was repeated thrice. The residue was then extracted in distilled water thrice and then washed in acetone to facilitate drying. The final purification was carried out on a preparative HPLC C18 column ($10 \times 250\text{mm}$, Phenomenex). HPLC conditions were as follows: solvent A, acetonitrile/TFA (100:0.1, v/v); solvent B, H₂O/TFA (100:0.1, v/v). Elution was done with the following mixtures: 40~45% solvent A (40 min), 45~65% solvent B (10 min). The flow rate was set to $3\text{ml}/\text{min}$ and the products were detected at 205nm . The soyasaponin I in this study was $>99\%$ pure as determined by an analytical HPLC C18 column ($4.6\text{mm} \times 250\text{mm}$, Phenomenex).

In vivo mouse model

We followed the guidelines for animal experimentation adopted by the Animal Subjects Program (ASP) at Taipei Veterans General Hospital (VGH-TPE). At the day of implantation, MOSEC cells (2×10^6) were injected into the abdominal/peritoneal cavity of 8 week old female C57BL/6 mice (National Laboratory Animal Center, Taipei, Taiwan). Alzet osmotic miniature pumps (model 1004; DURECT Corporation Charles River Laboratories, L'Arbresle, France) with constant delivery

rates of $0.11 \text{ l}/\text{h}$ for about 4 weeks were filled with either $100\mu\text{l}$ SsaI in PBS or DMSO as control. The pump had a delayed starting time of approximately 2 days after filling. The osmotic mini-pumps filled with either SsaI or DMSO were implanted under the skin of the mice under sterile conditions and started when no cartilage destruction was detectable (days 0-4). Since the reagents circulated for a few days after the pump was empty, an experimental setting of 28 days was selected.

Gene transfection

The lentiviral plasmid vectors harboring specific short hairpin RNA (shRNA) sequences for human ST3GalI and a non-target scrambled control were purchased from the RNAi Core Facility (Academia Sinica, Taiwan). The ST3GalI shRNA sequence was 5'-GCGGGAGAAGAAGCCCAATAA-3' (pLKO-TRC005 vector, Clone ID: TRCN0000231839). The ST3GalI shRNA or control plasmids (pLKO-TRC005 vector) were transduced into ovarian cancer cells with the lentivirus package plasmids using Lipofectamine 2000 (Invitrogen Life Technologies, Carlsbad, CA, USA) according to the manufacturer's instructions. Stable transfectants were selected in presence of $1\mu\text{g}/\text{ml}$ puromycin (Sigma-Aldrich, St Louis, MO, USA). For gain of function experiments, human ST3GalI expression plasmid (Origene, RC217696) and control plasmid (empty vector) was transfected using the GenJet plus *in vitro* DNA transfection kit (SignaGen, Maryland, USA).

RNA isolation and real-time quantitative PCR (RT-qPCR)

The ovarian cancer cells were lysed by TRIzol and centrifugation at $12,000 \times g$ for 10 minutes after adding bromochloropropane (Sigma-Aldrich). Total RNA was precipitated with isopropanol, followed by washing with ethanol to remove impurities and finally dissolved in RNAase-free water (Invitrogen). Total RNA was quantified spectrophotometrically using A260/A280 values. The cDNA synthesis was performed using SuperScript™ II reverse transcriptase (Invitrogen) according to the manufacturer's instructions. The $12\mu\text{L}$ volume of one reaction with oligo(dT)₁₂₋₁₈ ($500\mu\text{g}/\text{mL}$), $1\mu\text{L}$ dNTP Mix (10 mM each), 1 ng to $5\mu\text{g}$ total RNA and sterile distilled water to perform 65°C for 5 min and quick chill on ice. Add $7\mu\text{L}$ volume of buffer mix with 5X First-Strand Buffer, 0.1 M DTT and RNaseOUT™ (40 units/ μL) to perform 42°C for 2 min. Add $1\mu\text{L}$ (200 units) of SuperScript™ II RT to perform 42°C for 50 min and 70°C for 15 min. The PCR primers and probes designed using the Roche Online Assay Design Centre for the ST3GalI and EGFR genes and control 18S RNA were as follows: ST3GalI, Forward 5'- TGGTCCTGGAGCTCTCCGAGAA-3', Reverse 5'- GACTGTCTATCTCAGGCCCATAGAAGA-3';

EGFR, Forward 5'- ACTCATGCTCTACAACCC-3', Reverse 5'- CCAATACCTATTCCGTTACAC-3'; and 18S, Forward 5'-GACCAGAGCGAAAAGCAT-3', Reverse 5'-TCGGAACTACGACGGTATC-3'. The cDNA samples were amplified by real-time PCR using a LightCycler 480 Instrument (Roche). The 20 μ L volume of one reaction with 10ng/ μ L cDNA, 50nM Forward and Reverse primer, 2xSYBR reagent and sterile distilled water to perform PCR amplification and Melting curve program. Quantification cycle values (crossing point, Cp) for each gene were calculated as the cycle number at which the reporter fluorescence passed a fixed threshold above the base line. The expression levels of the genes of interest, ST3GalI and EGFR, were normalized in relation to the housekeeping control (18S). All experiments were performed thrice.

Protein isolation and western blot analysis

For western blot analysis, ovarian cancer cells that were treated with or without SsaI were lysed in a buffer containing 1% Triton X-100 in PBS and protease inhibitor mixture tablets (Roche, Barcelona, Spain). Following 30 min incubation on ice with vortexing, lysed cells were centrifuged (14000 rpm, 20 min, 4°C) to pellet cell debris, and protein concentrations of the resulting cell supernatants were determined by the Bradford Assay (Bio-Rad, Hemel Hempstead, UK), relative to a standard curve prepared from serial dilutions of bovine serum albumin (0–4mg/mL) with absorbance readings at 595nm. 100 μ g total protein was diluted in equal volumes of 2x protein sample buffer (125mM Tris-HCl (pH 6.8), 4% SDS, 0.02% bromophenol blue, 0.2M DTT, 20% glycerol) was electrophoresed on a 10% ~ 15% SDS-PAGE run 100 voltage, 3hrs and transferred onto Immobilon polyvinylidene difluoride membranes (Millipore, Bedford, MA) 90 voltage, 2hrs. Then, the membranes were incubated 30mins at room temperature in blocking solution (5% nonfat dry milk/0.1% Tween-20/1xPBS) followed by incubating the membranes overnight with the appropriate primary antibodies namely, ST3GalI (Abcam, ab96129, 1:500), EGFR (CST, #4267, 1:1000) or phospho-EGFR (CST, #2234, 1:1000). Then, the membranes were washed 10min trice with 0.05% Tween-20/PBS followed by incubation 2hrs at room temperature with anti-Rabbit HRP-conjugated secondary antibody (Genesland, #G701120, 1:5000). The blots were developed with enhanced chemiluminescence reagent (Amersham Pharmacia Biotech) followed by exposure to X-ray film to visualize the protein bands. The protein bands were quantitated using ImageJ analysis by determining the relative intensity for each experimental band by normalizing its absolute intensity to that of the control.

Immunohistochemistry

IHC specimens (59) from the CJ2 human ovarian cancer tissue array were obtained from a commercial

tissue array (Super Bio Chips, Seoul, S. Korea) with complete clinical data, including clinical stage, grade and overall survival (OS). Tissue sections were immersed in a coplin jar filled with 1x Dako target retrieval solution (Dako, Denmark; Code S1699), heated for 5 min at 121°C and then cooled to 85°C. Then, the endogenous peroxidase activity was quenched by treating the specimens with 0.6% hydrogen peroxide/methanol mix. The sections were further blocked with goat serum (BioGenex, San Ramon, CA, USA) for 30 min at room temperature to prevent non-specific binding. Then, the sections were incubated overnight with anti-ST3GalI Ab (Abcam, ab96129, 1:50) at 4°C followed by staining with AEC Substrate-Chromogen (DAKO, Denmark) and counterstained with hematoxylin. For the negative control, sections were treated with PBS instead of the antibody. The IHC staining was quantified based on the staining intensity score (0, no staining; 1, weak; 2, moderate; 3, strong). A strong intensity score indicated high expression of ST3GalI, whereas, other intensity scores indicated different grades of lower expression.

Duolink *In Situ* staining

Protein–protein interactions were detected using a Duolink *In Situ* Kit (Olink Bioscience, Uppsala, Sweden; PLA probe anti-rabbit plus; PLA probe anti-mouse minus; Detection Kit orange). In brief, tissue specimens from the *in vivo* mouse experiment were incubated with primary antibodies against ST3GalI and EGFR for 2h at room temperature. Then, the slides were washed twice in suitable buffer 1x wash buffer A (0.01 M Tris, 0.15 M NaCl and 0.05% Tween 20) for 5 min followed by incubation with the 2 PLA probes (1:5 in appropriate buffer antibody dilution) for 60 min at 37°C. Then, the specimens were incubated with ligase (1:40 in buffer high purity water). After washing twice in 1x wash buffer A for 2 min, the amplification procedure was carried out with the polymerase (1:80) for 100 min at 37°C. Then, the specimens were washed twice in 1x Wash Buffer B for 10 min and 0.01x Wash Buffer B for 1 min. The slides were finally incubated for 15 min with Oregon green phalloidin antibody (1:50, Invitrogen) at room temperature and visualized under a light microscope (Nikon, Ci).

Analysis of ovarian cancer and prognosis in the TCGA project

The clinical and protein expression data of ovarian cancer (high-grade serous cystadenocarcinoma) from the TCGA were downloaded from the Oncomine website (<http://www.oncomine.org/>). The patients in the ovarian serous cystadenocarcinoma dataset (Human Genome U133A array, 12,624 measured genes, 562 cases) were categorized using a total of 20 STs including α 2,3-, α 2,6-, and α 2,8-sialyltransferases with a tercile approach.

The patients were categorized as high or low expressing if the mRNA of interest was in the upper one-third or in the lower two-thirds, respectively. We analyzed the disease free survival (DFS), overall survival (OS) and the correlation between ST3GalII and EGFR using this dataset. Furthermore, different datasets (Schwartz ovarian, HumanGeneFL array [56]; Hendrix ovarian, Human Genome U133A array [57]; Denkart ovarian, Human Genome U133A array [58]; Lu ovarian, Human Genome U95 array, [59]) from the Oncomine website were used to investigate if ST3GalII regulated ovarian cancer dissemination. Further, the patients were sub-divided into either early stage (stages 1 and 2) or late stage (stages 3 and 4) and the expression of ST3GalII was compared between these 2 groups.

Microarray analysis

The microarray experiments were conducted using the L1000 Operating Procedure (L1000 SOP). In brief, a human ovarian cancer cell line, ES2, was grown in commercial 96-well plate for one day and the cells lysed with lysis buffer (L1000 kit) for 30 mins. The lysate was stored at 80°C overnight and then transferred to a 384-well plate for the L1000 assay that was conducted according to the commercial protocol (http://s3.amazonaws.com/support.lincsccloud.org/protocols/data_generation/L1000_SOP.pdf). Gene expression profiles in the control and study group were detected by L1000 array technology. Up and down probe sets were selected by 2-sample t-test with a *p* value lower than 0.01 and fold change greater than 1.5-fold considered as significant. The up and down probe sets were input into GeneE software to run the analysis and interpret the transcription profile data. The expression of sialylation and significant cell receptors, including EGFR, IGFR, VEGFR and PDGFR was determined.

Analysis of CCLE ovarian cancer and drug efficiency

The mRNA expression of ST3GalII-VI and the drug efficiency (Actarea) were derived from the cancer cell line encyclopedia (CCLE) ovarian cancer dataset (<https://portals.broadinstitute.org/ccle/home>). The TKI drugs included erlotinib, lapatinib, ZD-6474, and TKI258.

In Vitro cell viability assays

To assay the synergy between ST3GalII and EGFR, ES2 cells were treated with 100µM SsaI in presence or absence of EGFR inhibitor (Sigma, AG1478) in 96-well plates (4x10³ per well) and cultured for 48h. Then, the cells were collected and counted by staining a sample with trypan blue and the cell proliferation was measured with the MTT assay. Following 20µl of a sterile, filtered 3-(4, 5-dimethylthiazol-2-yl)-2, 5-diphenyltetrazolium bromide

(MTT) solution (5 mg/ml) in 1xPBS (pH 7.4) was added to each well and incubated for 4 hrs at 37°C, and adding 150µL dimethyl sulfoxide (DMSO) and incubating 10mins at 37°C. Absorbance was read at 560 nm on a microplate reader. The results were analyzed using the CompuSyn software (<http://www.combosyn.com/>). The IC₅₀ of each drug was determined by interpolation from the dose-response curves. The resulting combination index (CI) determined the quantitative degree of interaction between different drugs (CI=1 was denoted additivity; CI>1 was denoted antagonism; CI<1 was denoted synergism). For interpretation, the combination was plotted as Log₁₀ CI versus Fa (fraction affected defined as 1 – survival fraction). Based on these plots, additivity was defined as logCI = 0; synergy was defined as log₁₀ CI<0; antagonism was defined as log₁₀ CI>0.

Immunoprecipitation (IP)

Immunoprecipitation of ST3GalII and EGFR was performed using a Pierce Crosslink IP kit (#26147) according to the manufacturer's protocol. In brief, 10µg of Erbitux (Merck, 2mg/mL) antibody was coupled and cross-linked to protein A/G plus agarose resin (0.55mL of settled resin supplied as a 50% slurry). 1x10⁸ cells ES2-shST3GalII and ES2-scramble infected cells were rinsed with PBS, scraped and incubated in lysis buffer (0.025M Tris, 0.15M NaCl, 1mM EDTA, 1% NP40 and 5% glycerol supplemented with 1x EDTA-free protease inhibitor, Roche) for 1h at 4°C. The cell lysate was centrifuged at 10,000xg for 15min. The protein concentration in the supernatant was quantified (Bio-rad protein assay). Then, 1mg total protein was incubated with the cross-linked antibody overnight at 4°C. The immunoprecipitated proteins were washed trice with 200µL IP Lysis/Wash Buffer (0.025M Tris, 0.15M NaCl, 0.001M EDTA, 1% NP-40, 5% glycerol; pH 7.4), eluted with 60µL elution buffer (pH 2.8, contains primary amine) from protein A/G plus agarose resin binding identify EGFR protein column and resolved with 5x non-reducing lane marker sample Buffer (0.3M Tris-HCl, 5% SDS, 50% glycerol, lane marker tracking dye; pH 6.8) on a 12% SDS-PAGE. Then, western blot analysis was performed to detect either EGFR or ST3GalII using the appropriate antibodies previously mentioned (western blot section of methods).

Statistical analysis

Statistical analysis was performed using the SPSS software program. For cell invasion assay data, non-paired Student's t-test was used for comparisons between groups. The Kaplan-Meier survival curves were plotted for ovarian cancer patients and the *P* values were determined using the log-rank test for censored survival data. Survival time was censored if the patient was alive at the time of

evaluation. The relationship between IHC expression and other clinical or tumor parameters was calculated using the χ^2 test. A $P < 0.05$ was considered significant.

Author contributions

KC Wen and PH Wang performed the experiments and analyzed the data. KC Wen, PL Sung, SL Hsieh, YT Chou, OKS Lee, CW Wu and PH Wang contributed reagents/materials/analysis tools; KC Wen, SL Hsieh, and PH Wang wrote and revised the paper.

ACKNOWLEDGMENTS

This work was supported by grants from the Ministry of Science and Technology, Executive Yuan, Taiwan (NSC 99-2314-B-010-009-MY3; NSC 102-2314-B-010-032; MOST 103-2314-B-010-043-MY3; and MOST 103-2314-B-075-057-MY2), and Taipei Veterans General Hospital (V102C-141; V102E4-003; V103E4-003; V103C-112; V104C-095; V105C-096; V106C-129; V106D23-001-MY2-1; and CI-105-6). The funders had no role in study design, data collection and analysis, decision to publish, or preparation of the manuscript. We thank the Clinical Research Core Laboratory and the Medical Science & Technology Building of Taipei Veterans General Hospital for providing experimental space and facilities. We also thank Dr. Tsui-Ling Hsu (Genomics Research Center, Academia Sinica, Taipei, Taiwan) for her technical support.

CONFLICTS OF INTEREST

The authors declare that there is no conflict of interest.

REFERENCES

1. Siegel RL, Miller KD, Jemal A. Cancer statistics, 2016. *CA Cancer J Clin*. 2016; 66:7-30.
2. Sung PL, Jan YH, Lin SC, Huang CC, Lin H, Wen KC, Chao KC, Lai CR, Wang PH, Chuang CM, Wu HH, Twu NF, Yen MS, et al. Periostin in tumor microenvironment is associated with poor prognosis and platinum resistance in epithelial ovarian carcinoma. *Oncotarget*. 2016; 7:4036-4047. doi:10.18632/oncotarget.6700.
3. Lee WL, Chang WH, Wang KC, Guo CY, Chou YJ, Huang N, Huang HY, Yen MS, Wang PH. The Risk of Epithelial Ovarian Cancer of Women With Endometriosis May be Varied Greatly if Diagnostic Criteria Are Different: A Nationwide Population-Based Cohort Study. *Medicine (Baltimore)*. 2015; 94:e1633.
4. Horng HC, Lai CR, Chang WH, Wen KC, Chen YJ, Juang CM, Yen MS, Wang PH. Comparison of early-stage primary serous fallopian tube carcinomas and equivalent stage serous epithelial ovarian carcinomas. *Taiwan J Obstet Gynecol*. 2014; 53:547-551.
5. Hoskins P, Eisenhauer E, Vergote I, Dubuc-Lissoir J, Fisher B, Grimshaw R, Oza A, Plante M, Stuart G, Vermorken J. Phase II feasibility study of sequential couplets of Cisplatin/Topotecan followed by paclitaxel/cisplatin as primary treatment for advanced epithelial ovarian cancer: a National Cancer Institute of Canada Clinical Trials Group Study. *J Clin Oncol*. 2000; 18:4038-4044.
6. Herzog TJ, Pothuri B. Ovarian cancer: a focus on management of recurrent disease. *Nat Clin Pract Oncol*. 2006; 3:604-611.
7. Theriault C, Pinar M, Comamala M, Migneault M, Beaudin J, Matte I, Boivin M, Piche A, Rancourt C. MUC16 (CA125) regulates epithelial ovarian cancer cell growth, tumorigenesis and metastasis. *Gynecol Oncol*. 2011; 121:434-443.
8. Harduin-Lepers A, Recchi MA, Delannoy P. 1994, the year of sialyltransferases. *Glycobiology*. 1995; 5:741-758.
9. Warren L, Fuhrer JP, Buck CA. Surface glycoproteins of normal and transformed cells: a difference determined by sialic acid and a growth-dependent sialyl transferase. *Proc Natl Acad Sci U S A*. 1972; 69:1838-1842.
10. Pilatte Y, Bignon J, Lambre CR. Sialic acids as important molecules in the regulation of the immune system: pathophysiological implications of sialidases in immunity. *Glycobiology*. 1993; 3:201-218.
11. Wang PH, Li YF, Juang CM, Lee YR, Chao HT, Ng HT, Tsai YC, Yuan CC. Expression of sialyltransferase family members in cervix squamous cell carcinoma correlates with lymph node metastasis. *Gynecol Oncol*. 2002; 86:45-52.
12. Harduin-Lepers A, Mollicone R, Delannoy P, Oriol R. The animal sialyltransferases and sialyltransferase-related genes: a phylogenetic approach. *Glycobiology*. 2005; 15:805-817.
13. Krzewinski-Recchi MA, Julien S, Juliant S, Teinturier-Lelievre M, Samyn-Petit B, Montiel MD, Mir AM, Cerutti M, Harduin-Lepers A, Delannoy P. Identification and functional expression of a second human beta-galactoside alpha2,6-sialyltransferase, ST6Gal II. *Eur J Biochem*. 2003; 270:950-961.
14. Takashima S, Tsuji S, Tsujimoto M. Characterization of the second type of human beta-galactoside alpha 2,6-sialyltransferase (ST6Gal II), which sialylates Galbeta 1,4GlcNAc structures on oligosaccharides preferentially. Genomic analysis of human sialyltransferase genes. *J Biol Chem*. 2002; 277:45719-45728.
15. Huang S, Day TW, Choi MR, Safa AR. Human beta-galactoside alpha-2,3-sialyltransferase (ST3GalIII) attenuated Taxol-induced apoptosis in ovarian cancer cells by downregulating caspase-8 activity. *Mol Cell Biochem*. 2009; 331:81-88.
16. Wang PH, Lee WL, Juang CM, Yang YH, Lo WH, Lai CR, Hsieh SL, Yuan CC. Altered mRNA expressions of sialyltransferases in ovarian cancers. *Gynecol Oncol*. 2005; 99:631-639.

17. Christie DR, Shaikh FM, Lucas JAt, Lucas JA, 3rd and Bellis SL. ST6Gal-I expression in ovarian cancer cells promotes an invasive phenotype by altering integrin glycosylation and function. *J Ovarian Res.* 2008; 1:3.
18. Wu CY, Hsu CC, Chen ST, Tsai YC. Soyasaponin I, a potent and specific sialyltransferase inhibitor. *Biochem Biophys Res Commun.* 2001; 284:466-469.
19. Hsu CC, Lin TW, Chang WW, Wu CY, Lo WH, Wang PH, Tsai YC. Soyasaponin-I-modified invasive behavior of cancer by changing cell surface sialic acids. *Gynecol Oncol.* 2005; 96:415-422.
20. Chang WW, Yu CY, Lin TW, Wang PH, Tsai YC. Soyasaponin I decreases the expression of alpha2,3-linked sialic acid on the cell surface and suppresses the metastatic potential of B16F10 melanoma cells. *Biochem Biophys Res Commun.* 2006; 341:614-619.
21. Kaszuba K, Grzybek M, Orłowski A, Danne R, Rog T, Simons K, Coskun U, Vattulainen I. N-Glycosylation as determinant of epidermal growth factor receptor conformation in membranes. *Proc Natl Acad Sci U S A.* 2015; 112:4334-4339.
22. Yarden Y, Sliwkowski MX. Untangling the ErbB signalling network. *Nat Rev Mol Cell Biol.* 2001; 2:127-137.
23. Yarden Y, Pines G. The ERBB network: at last, cancer therapy meets systems biology. *Nat Rev Cancer.* 2012; 12:553-563.
24. Ricci F, Fratelli M, Guffanti F, Porcu L, Spriano F, Dell'Anna T, Fruscio R, Damia G. Patient-derived ovarian cancer xenografts re-growing after a cisplatin treatment are less responsive to a second drug re-challenge: a new experimental setting to study response to therapy. *Oncotarget.* 2017;8:7441-7451.doi:10.18632/oncotarget.7465.
25. Remon J, Besse B. Unravelling signal escape through maintained EGFR activation in advanced non-small cell lung cancer (NSCLC): new treatment options. *ESMO Open.* 2016; 1:e000081.
26. Morgillo F, Della Corte CM, Fasano M, Ciardiello F. Mechanisms of resistance to EGFR-targeted drugs: lung cancer. *ESMO Open.* 2016; 1:e000060.
27. Ciardiello F, Tortora G. EGFR antagonists in cancer treatment. *N Engl J Med.* 2008; 358:1160-1174.
28. Ferguson KM. Structure-based view of epidermal growth factor receptor regulation. *Annu Rev Biophys.* 2008; 37:353-373.
29. Zhao J, Klausen C, Qiu X, Cheng JC, Chang HM, Leung PC. Betacellulin induces Slug-mediated down-regulation of E-cadherin and cell migration in ovarian cancer cells. *Oncotarget.* 2016; 7:28881-28890.doi: 10.18632/oncotarget.7591.
30. Yen HY, Liu YC, Chen NY, Tsai CF, Wang YT, Chen YJ, Hsu TL, Yang PC, Wong CH. Effect of sialylation on EGFR phosphorylation and resistance to tyrosine kinase inhibition. *Proc Natl Acad Sci U S A.* 2015; 112:6955-6960.
31. Park JJ, Yi JY, Jin YB, Lee YJ, Lee JS, Lee YS, Ko YG, Lee M. Sialylation of epidermal growth factor receptor regulates receptor activity and chemosensitivity to gefitinib in colon cancer cells. *Biochem Pharmacol.* 2012; 83:849-857.
32. Granados ML, Hudson LG, Samudio-Ruiz SL. Contributions of the Epidermal Growth Factor Receptor to Acquisition of Platinum Resistance in Ovarian Cancer Cells. *PLoS One.* 2015; 10:e0136893.
33. Wang SQ, Liu ST, Zhao BX, Yang FH, Wang YT, Liang QY, Sun YB, Liu Y, Song ZH, Cai Y, Li GF. Afatinib reverses multidrug resistance in ovarian cancer via dually inhibiting ATP binding cassette subfamily B member 1. *Oncotarget.* 2015; 6:26142-26160.doi: 10.18632/oncotarget.4536.
34. Siwak DR, Carey M, Hennessy BT, Nguyen CT, McGahren Murray MJ, Nolden L, Mills GB. Targeting the epidermal growth factor receptor in epithelial ovarian cancer: current knowledge and future challenges. *J Oncol.* 2010; 2010:568938.
35. Psyrri A, Kassar M, Yu Z, Bamias A, Weinberger PM, Markakis S, Kowalski D, Camp RL, Rimm DL, Dimopoulos MA. Effect of epidermal growth factor receptor expression level on survival in patients with epithelial ovarian cancer. *Clin Cancer Res* 2005; 11:8637-8643.
36. Gui T, Shen K. The epidermal growth factor receptor as a therapeutic target in epithelial ovarian cancer. *Cancer Epidemiol.* 2012; 36:490-496.
37. Hakomori S. Aberrant glycosylation in tumors and tumor-associated carbohydrate antigens. *Adv Cancer Res.* 1989; 52:257-331.
38. Harduin-Lepers A, Vallejo-Ruiz V, Krzewinski-Recchi MA, Samyn-Petit B, Julien S, Delannoy P. The human sialyltransferase family. *Biochimie.* 2001; 83:727-737.
39. Dall'Olivo F, Chiricolo M. Sialyltransferases in cancer. *Glycoconj J.* 2001; 18:841-850.
40. Kannagi R. Carbohydrate-mediated cell adhesion involved in hematogenous metastasis of cancer. *Glycoconj J.* 1997; 14:577-584.
41. Kitagawa H, Paulson JC. Cloning and expression of human Gal beta 1,3(4)GlcNAc alpha 2,3-sialyltransferase. *Biochem Biophys Res Commun.* 1993; 194:375-382.
42. Gillespie W, Kelm S, Paulson JC. Cloning and expression of the Gal beta 1, 3GalNAc alpha 2,3-sialyltransferase. *J Biol Chem.* 1992; 267:21004-21010.
43. Burchell J, Poulsom R, Hanby A, Whitehouse C, Cooper L, Clausen H, Miles D, Taylor-Papadimitriou J. An alpha2,3 sialyltransferase (ST3GalI) is elevated in primary breast carcinomas. *Glycobiology.* 1999; 9:1307-1311.
44. Videira PA, Correia M, Malagolini N, Crespo HJ, Ligeiro D, Calais FM, Trindade H, Dall'Olivo F. ST3Gal.I sialyltransferase relevance in bladder cancer tissues and cell lines. *BMC Cancer.* 2009; 9:357.

45. Kudo T, Ikehara Y, Togayachi A, Morozumi K, Watanabe M, Nakamura M, Nishihara S, Narimatsu H. Up-regulation of a set of glycosyltransferase genes in human colorectal cancer. *Lab Invest.* 1998; 78:797-811.
46. Konoshima T, Kokumai M, Kozuka M, Tokuda H, Nishino H, Iwashima A. Anti-tumor-promoting activities of afromosin and soyasaponin I isolated from *Wistaria brachybotrys*. *J Nat Prod.* 1992; 55:1776-1778.
47. Citri A, Yarden Y. EGF-ERBB signalling: towards the systems level. *Nat Rev Mol Cell Biol.* 2006; 7:505-516.
48. Morandell S, Stasyk T, Skvortsov S, Ascher S, Huber LA. Quantitative proteomics and phosphoproteomics reveal novel insights into complexity and dynamics of the EGFR signaling network. *Proteomics.* 2008; 8:4383-4401.
49. Camidge DR, Pao W and Sequist LV. Acquired resistance to TKIs in solid tumours: learning from lung cancer. *Nat Rev Clin Oncol.* 2014; 11:473-481.
50. Niederst MJ, Engelman JA. Bypass mechanisms of resistance to receptor tyrosine kinase inhibition in lung cancer. *Sci Signal.* 2013; 6:re6.
51. Yokoe S, Takahashi M, Asahi M, Lee SH, Li W, Osumi D, Miyoshi E, Taniguchi N. The Asn418-linked N-glycan of ErbB3 plays a crucial role in preventing spontaneous heterodimerization and tumor promotion. *Cancer research.* 2007; 67:1935-1942.
52. Whitson KB, Whitson SR, Red-Brewer ML, McCoy AJ, Vitali AA, Walker F, Johns TG, Beth AH, Staros JV. Functional effects of glycosylation at Asn-579 of the epidermal growth factor receptor. *Biochemistry.* 2005; 44:14920-14931.
53. Tsuda T, Ikeda Y, Taniguchi N. The Asn-420-linked sugar chain in human epidermal growth factor receptor suppresses ligand-independent spontaneous oligomerization. Possible role of a specific sugar chain in controllable receptor activation. *J Biol Chem.* 2000; 275:21988-21994.
54. Liu YC, Yen HY, Chen CY, Chen CH, Cheng PF, Juan YH, Chen CH, Khoo KH, Yu CJ, Yang PC, Hsu TL, Wong CH. Sialylation and fucosylation of epidermal growth factor receptor suppress its dimerization and activation in lung cancer cells. *Proc Natl Acad Sci U S A.* 2011; 108:11332-11337.
55. Takai N, Ueda T, Nishida M, Nasu K, Narahara H. Synergistic anti-neoplastic effect of AG1478 in combination with cisplatin or paclitaxel on human endometrial and ovarian cancer cells. *Mol Med Rep.* 2010; 3:479-484.
56. Schwartz DR, Kardia SL, Shedden KA, Kuick R, Michailidis G, Taylor JM, Misek DE, Wu R, Zhai Y, Darrah DM, Reed H, Ellenson LH, Giordano TJ, et al. Gene expression in ovarian cancer reflects both morphology and biological behavior, distinguishing clear cell from other poor-prognosis ovarian carcinomas. *Cancer research.* 2002; 62:4722-4729.
57. Hendrix ND, Wu R, Kuick R, Schwartz DR, Fearon ER, Cho KR. Fibroblast growth factor 9 has oncogenic activity and is a downstream target of Wnt signaling in ovarian endometrioid adenocarcinomas. *Cancer research.* 2006; 66:1354-1362.
58. Denkert C, Budczies J, Darb-Esfahani S, Györfy B, Sehouli J, Konsgen D, Zeillinger R, Weichert W, Noske A, Buckendahl AC, Müller BM, Dietel M, Lage H. A prognostic gene expression index in ovarian cancer-validation across different independent data sets. *The Journal of pathology.* 2009; 218:273-280.
59. Lu KH, Patterson AP, Wang L, Marquez RT, Atkinson EN, Baggerly KA, Ramoth LR, Rosen DG, Liu J, Hellstrom I, Smith D, Hartmann L, Fishman D, et al. Selection of potential markers for epithelial ovarian cancer with gene expression arrays and recursive descent partition analysis. *Clin Cancer Res* 2004; 10:3291-3300.